Supporting Information for:

Polysulfobetaine-based diblock copolymer nano-objects *via* polymerization-induced self-assembly

Kay E. B. Doncom, Nicholas J. Warren and Steven P. Armes

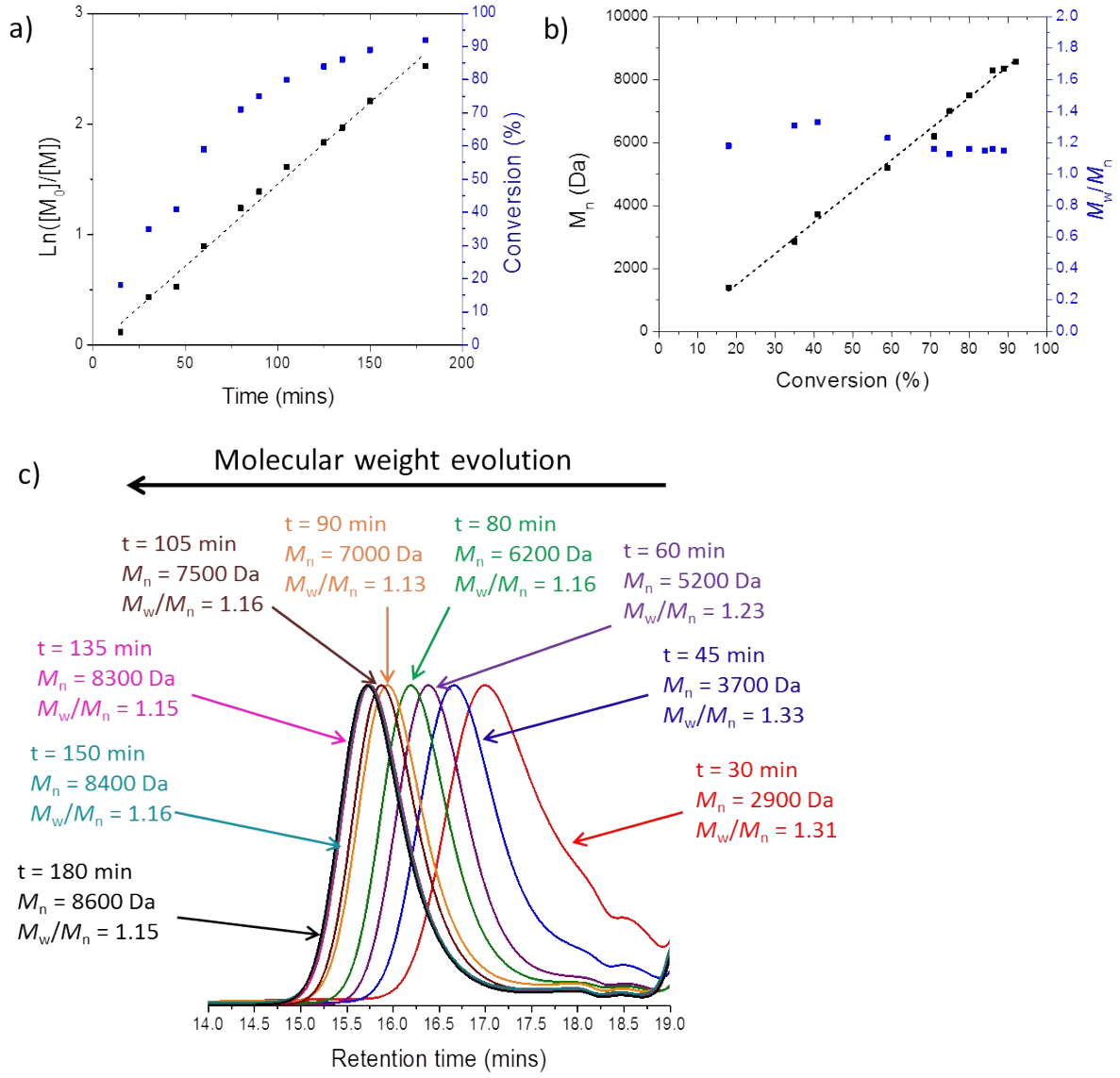

Figure S1. (a) Kinetics of the polymerization of SBMA using a 4-cyanopentanoic acid dithiobenzoate chain transfer agent at 70 °C. Approximately 90% conversion is achieved within 3 h and the semi-logarithmic plot exhibits a linear relationship. (b) Evolution of molecular weight (M_n) and M_w/M_n with conversion. (c) Gel permeation chromatograms (phosphate buffer eluent, refractive index detector) obtained for the kinetics of polymerization of SBMA using 4-cyanopentanoic acid dithiobenzoate at 70 °C. Calibration was achieved using a series of near-monodisperse poly(ethylene oxide) standards.

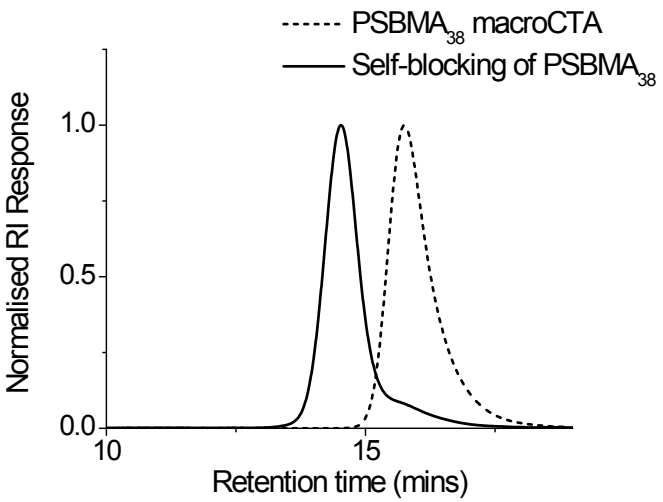

Figure S2. Gel permeation chromatogram curves (phosphate buffer eluent, refractive index detector) obtained for the 'self-blocking' chain extension of $PSBMA_{38}$ using 100 units of SBMA monomer at 70 °C. Calibration was achieved using a series of near-monodisperse poly(ethylene oxide) standards.

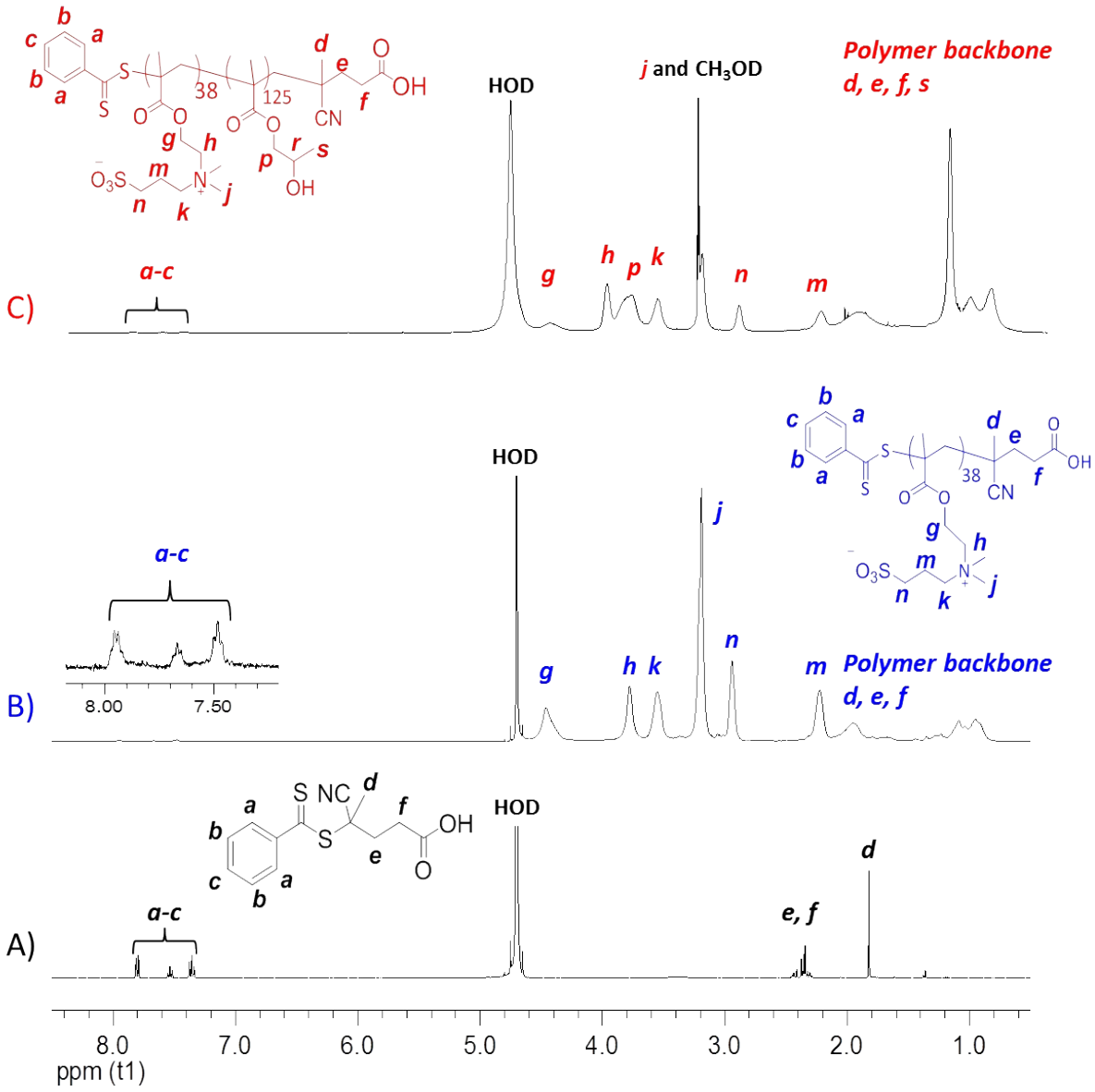

Figure S3. ^{1}H NMR spectra recorded for (A) CADB CTA in D_2O, (B) $PSBMA_{38}$ macro-CTA in D_2O, (C) $PSBMA_{38}$-$PHPMA_{125}$ diblock copolymer dissolved in a 50:50 v/v mixture of D_2O and CD_3OD.

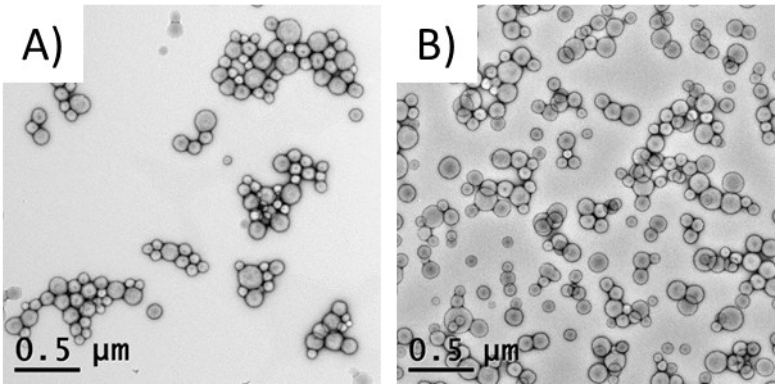

Figure S4. Representative TEM images obtained for (A) $PSBMA_{38}$-$PHPMA_{400}$ vesicles dispersed in water after 1 week (D_{TEM} = 119 ± 27 nm) and (B) $PSBMA_{38}$-$PHPMA_{400}$ vesicles dispersed in 1M $MgSO_4$ solution after 1 week (D_{TEM} = 116 ± 31 nm). The scale bar in both images is 0.5 µm. Clearly, the addition of salt has not had any discernible effect on the copolymer morphology.

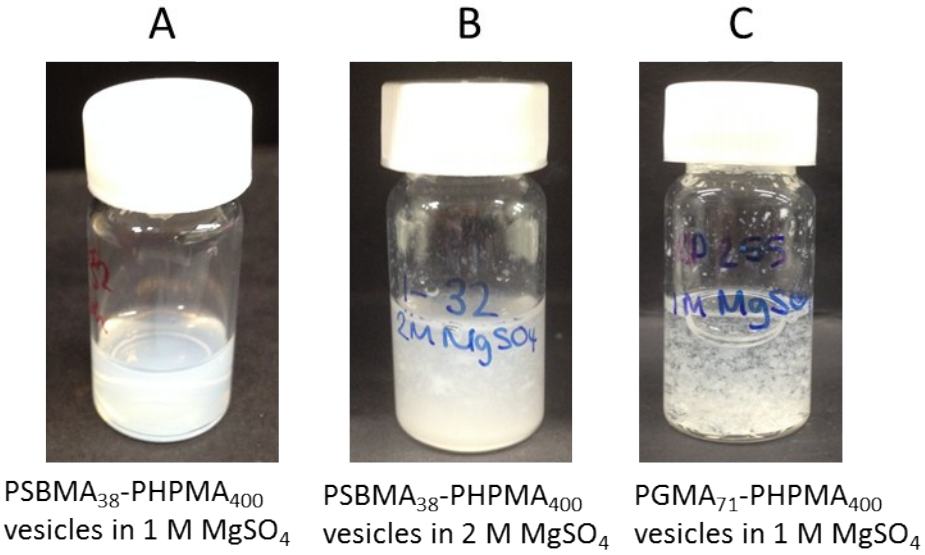

Figure S5. Digital photographs of (A) $PSBMA_{38}$-$PHPMA_{400}$ vesicles in 1 M $MgSO_4$ solution, (B) $PSBMA_{38}$-$PHPMA_{400}$ vesicles in 2 M $MgSO_4$ solution, (C) $PGMA_{71}$-$PHPMA_{400}$ vesicles in 1 M $MgSO_4$ solution.

Table S1: Characterization obtained for S_{38}-H_X-Y diblock copolymer dispersions, used to construct the phase diagram shown in Figure 4 in the main article.

Diblock composition	Solids content (% w/w)	Target DP	Conv. (%)	Actual DP	Z-average (nm)	DLS PDI	TEM morphology
S_{38}-H_{201}-10	10	201	> 99	201	40	0.09	S
S_{38}-H_{304}-10	10	304	> 99	304	39	0.15	S
S_{38}-H_{403}-10	10	403	> 99	403	62	0.09	S
S_{38}-H_{313}-12.5	12.5	316	99	313	58	0.11	S
S_{38}-H_{396}-12.5	12.5	400	99	396	111	0.05	S, V
S_{38}-H_{286}-13.5	13.5	289	99	286	155	127	S, V
S_{38}-H_{302}-13.5	13.5	302	> 99	302	140	0.04	S, V
S_{38}-H_{150}-14	14	150	> 99	150	22	0.2	S
S_{38}-H_{249}-14	14	249	> 99	249	132	91	S, W, V
S_{38}-H_{127}-15	15	127	> 99	127	58	0.28	S
S_{38}-H_{152}-15	15	155	98	152	38	0.4	S, W
S_{38}-H_{200}-15	15	200	> 99	200	95	0.2	S, W
S_{38}-H_{215}-15	15	215	> 99	215	104	0.19	S, W
S_{38}-H_{246}-15	15	248	99	246	126	0.11	S, W, V
S_{38}-H_{323}-15	15	325	99	323	334	0.16	S, V
S_{38}-H_{341}-15	15	348	98	341	188	0.03	S, V
S_{38}-H_{400}-15	15	400	> 99	400	157	0.04	S, V
S_{38}-H_{189}-16	16	189	> 99	189	273	0.26	S, W
S_{38}-H_{200}-16	16	200	> 99	200	325	0.28	W
S_{38}-H_{213}-16	16	215	99	213	411	0.29	W
S_{38}-H_{230}-16	16	230	> 99	230	411	0.28	W, V
S_{38}-H_{251}-16	16	251	> 99	251	352	0.26	S, W, V
S_{38}-H_{270}-16	16	270	> 99	270	375	0.08	S, V
S_{38}-H_{287}-16	16	290	99	287	297	0.13	S, V
S_{38}-H_{323}-16	16	323	> 99	323	267	0.04	S, V
S_{38}-H_{205}-17.5	17.5	205	> 99	205	288	0.25	W
S_{38}-H_{217}-17.5	17.5	217	> 99	217	541	0.27	W
S_{38}-H_{224}-17.5	17.5	224	> 99	224	363	0.3	W
S_{38}-H_{260}-17.5	17.5	260	> 99	260	200	0.15	V
S_{38}-H_{279}-17.5	17.5	279	> 99	279	475	0.16	V
S_{38}-H_{281}-17.5	17.5	281	> 99	281	523	0.12	V
S_{38}-H_{303}-17.5	17.5	303	> 99	303	359	0.18	V
S_{38}-H_{352}-17.5	17.5	352	> 99	352	238	0.19	V

Diblock composition	Solids content (% w/w)	Target DP	Conv (%)	Actual DP	Z-average (nm)	DLS PDI	TEM morphology
S_{38}-H_{125}-20	20	125	> 99	125	73	0.3	S
S_{38}-H_{150}-20	20	150	> 99	150	570	0.82	S
S_{38}-H_{200}-20	20	200	> 99	200	420	0.29	W
S_{38}-H_{223}-20	20	225	99	223	440	0.22	W, V
S_{38}-H_{250}-20	20	250	> 99	250	307	0.4	W, V
S_{38}-H_{310}-20	20	310	> 99	310	202	0.12	V
S_{38}-H_{366}-20	20	366	> 99	366	146	0.03	V
S_{38}-H_{392}-20	20	400	98	392	190	0.04	V
S_{38}-H_{191}-22.5	22.5	191	> 99	191	nd	nd	W
S_{38}-H_{115}-25	25	115	> 99	115	30	0.34	W
S_{38}-H_{128}-25	25	128	> 99	128	34	0.25	S, W
S_{38}-H_{139}-25	25	140	99	139	43	0.35	S, W
S_{38}-H_{150}-25	25	150	> 99	150	100	0.54	S, W
S_{38}-H_{180}-25	25	180	> 99	180	nd	nd	S, W
S_{38}-H_{188}-25	25	190	99	188	nd	nd	W
S_{38}-H_{196}-25	25	198	99	196	526	0.26	W, V
S_{38}-H_{204}-25	25	204	> 99	204	254	0.48	W, V
S_{38}-H_{221}-25	25	225	98	221	326	0.28	W, V
S_{38}-H_{233}-25	25	235	99	233	682	347	W, V
S_{38}-H_{240}-25	25	240	> 99	240	1020	0.19	W, V
S_{38}-H_{252}-25	25	252	> 99	252	347	0.38	V
S_{38}-H_{300}-25	25	300	> 99	300	202	0.15	V
S_{38}-H_{400}-25	25	400	> 99	400	246	0.06	V